Observations with Moored Acoustic Doppler Current Profilers in the Convection Regime in the Golfe du Lion

FRIEDRICH SCHOTT

Institut für Meereskunde an der Universität Kiel, Kiel, Federal Republic of Germany

KEVIN D. LEAMAN

Rosenstiel School of Marine and Atmospheric Sciences, University of Miami, Miami, Florida

(Manuscript received 1 September 1989, in final form 2 July 1990)

ABSTRACT

In the Golfe du Lion, south of France, favorable conditions for deep winter convection exist and were documented by the MEDOC experiments during 1969–75. A renewed investigation of that regime with upward-looking moored acoustic Doppler current profilers (ADCPs) was carried out during 24 January–5 March 1987, to record the three-dimensional currents associated with the deep mixing. While in the earlier studies initial deep convection did not begin until fairly late in the winter season, a very strong Mistral around 10 January 1987 had already generated a large deep-mixed patch, homogeneous down to around 2000 m at deployment time. Three ADCPs, two working at 150 kHz and one at 75 kHz, were moored in a triangle of 15 km sidelength at 550–780 m depth. Full records at 1-hour ensemble time intervals, 400 pings per ensemble, 8 m bin lengths were obtained by the 75 kHz and one of the 150 kHz ADCPs.

In mid-February, a second Mistral hit the region. With the onset of strong winds and surface cooling the occurrence of short-period current fluctuations, in the period range of hours, was observed which lasted for the duration of the negative heat flux.

The vertical currents recorded by the ADCPs during this period included downward events of 5–10 cm s^{-1} velocity with weaker upward motion in between. These events appeared to occur simultaneously over the depth range of several 100 m covered by the ADCPs. An interpretation of these events as frozen structures, advected by with the mean current, yielded a horizontal scale estimate of only order 1 km. The mean vertical velocity during the Mistral week due to the integrated effect of these events was of order 1 cm s^{-1} downward.

1. Introduction

In the Golfe du Lion, south of France, three factors combine to make this a preferred region of winter deep convection. First, the wintertime circulation is cyclonic, i.e., isopycnals show a doming in the center, with basically a three-layer stratification: a surface layer of relatively low salinity ($S < 38.3‰$) overlies an intermediate warm salty layer ($S > 38.5‰$) of eastern Mediterranean water in the depth range 200–600 m and deep water of about constant properties ($S \approx 38.43‰$) underneath; stratification underneath the surface layer is weak (Swallow and Gaston 1973). Second, the topography of the Rhône fan seems to trap the cyclonic circulation, making it fairly predictable where the center of the dome will appear in each winter season (Hogg 1973). Third, two types of cold and dry winds off the continent frequently blow over this cyclonic circulation feature in winter: The "Mistral" out of the Rhône valley and the "Tramontane" from along the north side of the Pyrenees. The paths of both winds cross over the center of the isopycnical dome.

The effect of either wind is to increase cooling and evaporation, which can lead to enough of a density increase of the surface layer that it reaches and exceeds the density of the weakly stratified sublayer. Evidence for vigorous convection has been observed associated with this breakthrough process in a series of experiments initiated by the so-called MEDOC Group. Deep convection was observed in 1969 (MEDOC Group 1970), in 1970 and in 1975, while it did not occur in 1972 (Gascard 1973, 1978). Besides observing the consequences of deep convection by a sequence of hydrographic surveys, these experiments saw the first application of a novel technology to measure directly the vertical currents with deep floats (Voorhis and Webb 1970) which were held at a certain pressure level by their compressibility and equipped with rotor fins which made them turn when the water was flowing upwards or downwards past them. During the stratified phase, upwelling in the order of 1 mm s^{-1} was measured with these rotating floats (Gascard 1978) in the

Corresponding author address: Dr. Friedrich Schott, Institut für Meereskunde an der Universität Kiel, Düsternbrooker Weg 20, F.R. Germany.

cyclonically rotating regime and also independently estimated from evaluation of the density conservation equation by Seung (1980). During the downbursts following the onset of strong Mistral winds, velocities of more than 5 cm s^{-1} were measured with the rotating float method.

With the emergence of self-contained acoustic Doppler current profilers (ADCPs), a technique is now available in which profiles of the three-dimensional Doppler currents can be measured over a range of hundreds of meters with reasonable time resolution, and with an accuracy that should permit measurements of vertical velocity signals occurring during convection events.

To obtain time series of currents in the convection regime, an array of three moorings with upward-looking ADCPs on top was deployed in the Golfe du Lion during 24 January to 5 March 1987 (Fig. 1a). Shipboard measurements with CTD hydrography and PEGASUS profiling were carried out aboard R/V *Columbus Iselin* several times during the experiment. A first brief account of this experiment was given by Schott et al. (1988), and an evaluation of the surface signal of the upward ADCPs in relation to wind speed and direction was given by Schott (1989).

This paper presents the results of the moored ADCPs and of the conventional current meters deployed underneath, in relation to meteorological observations obtained by coastal stations and on the *Iselin,* while the shipboard hydrographic measurements and heat flux calculations are discussed elsewhere (Leaman and Schott 1991, called LS in the following.

Unfortunately, whereas in the earlier MEDOC studies the breakthrough of the mixed layer occurred between late January and early March, this process had already taken place when we appeared on the scene on 22 January 1987. An exceptionally strong Mistral with snowfall along the Côte d'Azur occurred on 11/12 January (Fig. 2a,b) and most likely the deep convection happened at this time.

In the following we show some of the relevant environmental data, then describe the moored ADCP experiment and briefly discuss the acoustical data analysis and quality. We then focus on the processes during the Mistral period 15–22 February when several short-period downward velocity bursts occur. These downward motions, while not correlated over the separation of the moorings were almost homogeneous over the entire view range of the ADCPs and, in conjunction with the horizontal currents, allow some conclusions to be drawn regarding their three-dimensional characteristics.

2. Meteorological and hydrographic conditions

a. Meteorology

Meteorological data were obtained from three sources:

- hourly wind and air temperature data from French coastal stations Cape Bear, Sete, Cape Couronne and Pomegues (Fig. 1a);
- high-resolution wind, air and water temperatures logged on the SAIL system of R/V *Iselin;* however, these are from over the observation site only for part of the time;
- 12-hourly wind stress, air temperature and heat flux components from the French PERIDOT model which has a horizontal resolution of 35 km.

All four coastal stations show the coldest air temperatures in mid-January and they also show two other cold air outbreaks, in late December 1986 and in mid-February 1987 (Fig. 2b). In the December and February events the winds are towards the SSE at all stations, over extended periods of time while the event of mid-January, which had the highest wind speeds, was of only a few days duration and more nonhomogeneous among the stations (Fig. 2a).

Meteorological conditions for deep convection were most favorable around 10–15 January when the coldest air temperatures occurred simultaneously with the highest wind speed. An earlier if weaker possibility, with temperatures near the freezing point at station Pomegues, just north of the cyclonic dome, existed already at around 25-27 December (Fig. 2b); but winds then were significantly below those of the January event (Fig. 2a).

Winds recorded by R/V *Iselin* when within about 100 km of the mooring site agree well with those from the coastal station Pomegues nearby (Fig. 2c). The mid-February Mistral began with a wind speed increase and temperature decrease (Pomegues, Fig. 2c,d) on 15 February. Heat flux of the PERIDOT model (discussed in LS) from a grid point over the observation site begins to decrease on 13/14 February (Fig. 2e). Minimum temperatures (Fig. 2d), and maximum heat loss occur around 20 February. During 20–24 February, temperatures gradually rise back to normal (Fig. 2d), but the heat loss already decreases drastically between 20 and 22 February. The reason is the decrease of sensible and latent heat loss due to the wind speed decrease after 20 February. Therefore, in the analysis of what is called subsequently the "Mistral week", we will use the period 15–22 February.

b. Hydrography

We arrived in the observational area on 23 January, after initial breakthrough of the stratification had already taken place and a large deep-mixed patch had developed (Fig. 3a). As examples of the stratification outside and within the deep-mixed patch, two CTD profiles are shown in Fig. 4 (for details of the hydrographic discussion we refer to LS). Potential temperature and salinity for station U7 (CTD cast 20), outside the deep-mixed patch, still shows the three-layered distribution with the intermediate salinity maximum (Fig.

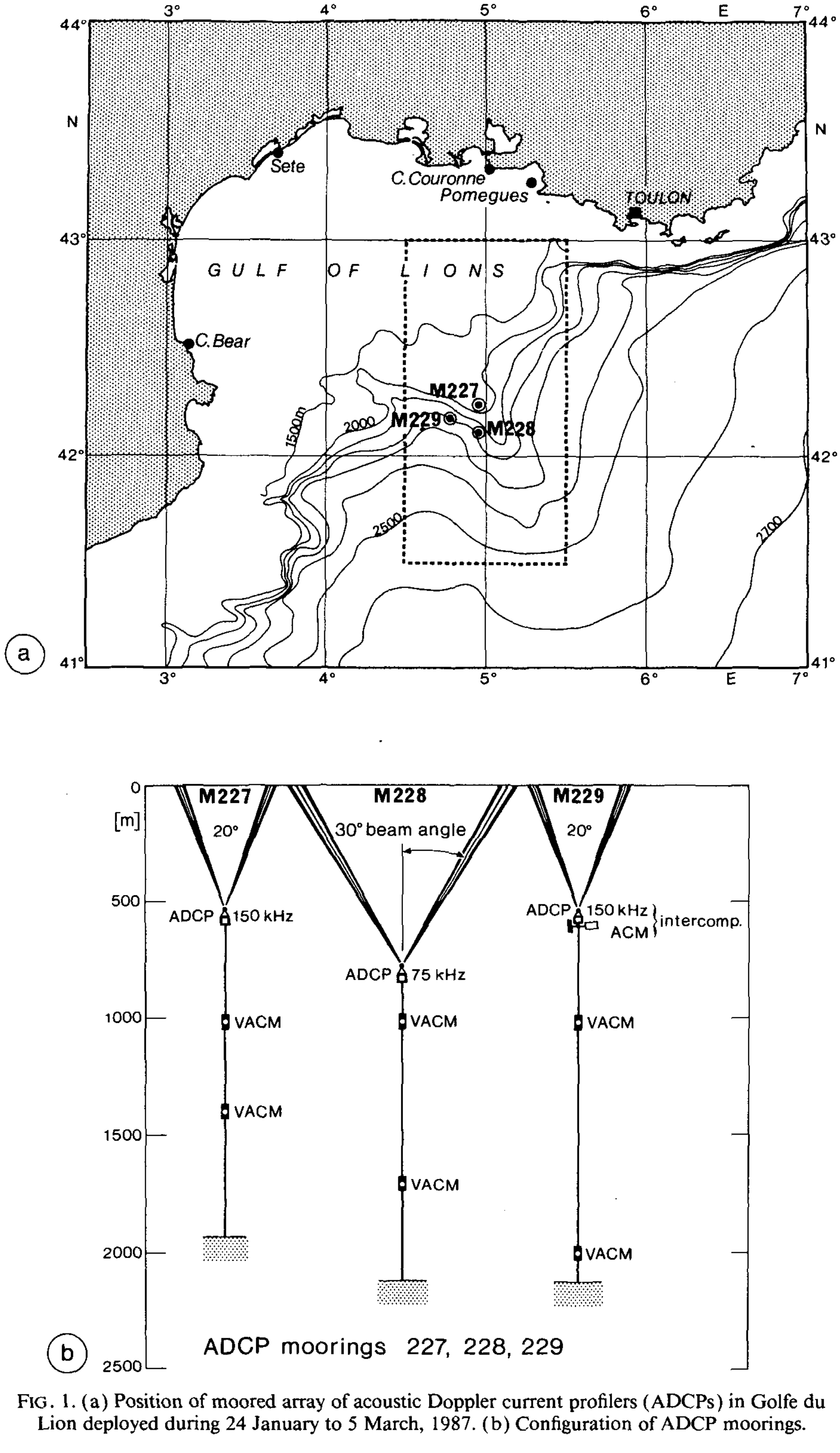

FIG. 1. (a) Position of moored array of acoustic Doppler current profilers (ADCPs) in Golfe du Lion deployed during 24 January to 5 March, 1987. (b) Configuration of ADCP moorings.

4) as described in the introduction, while station U4 (cast 23), near the position of mooring M227 in the center of the deep-mixed patch shows homogeneity down to the bottom at 2000 m. The sharp front between the stratified and unstratified regime, located at 41°45′N along 5°E late on 23 January moved gradually

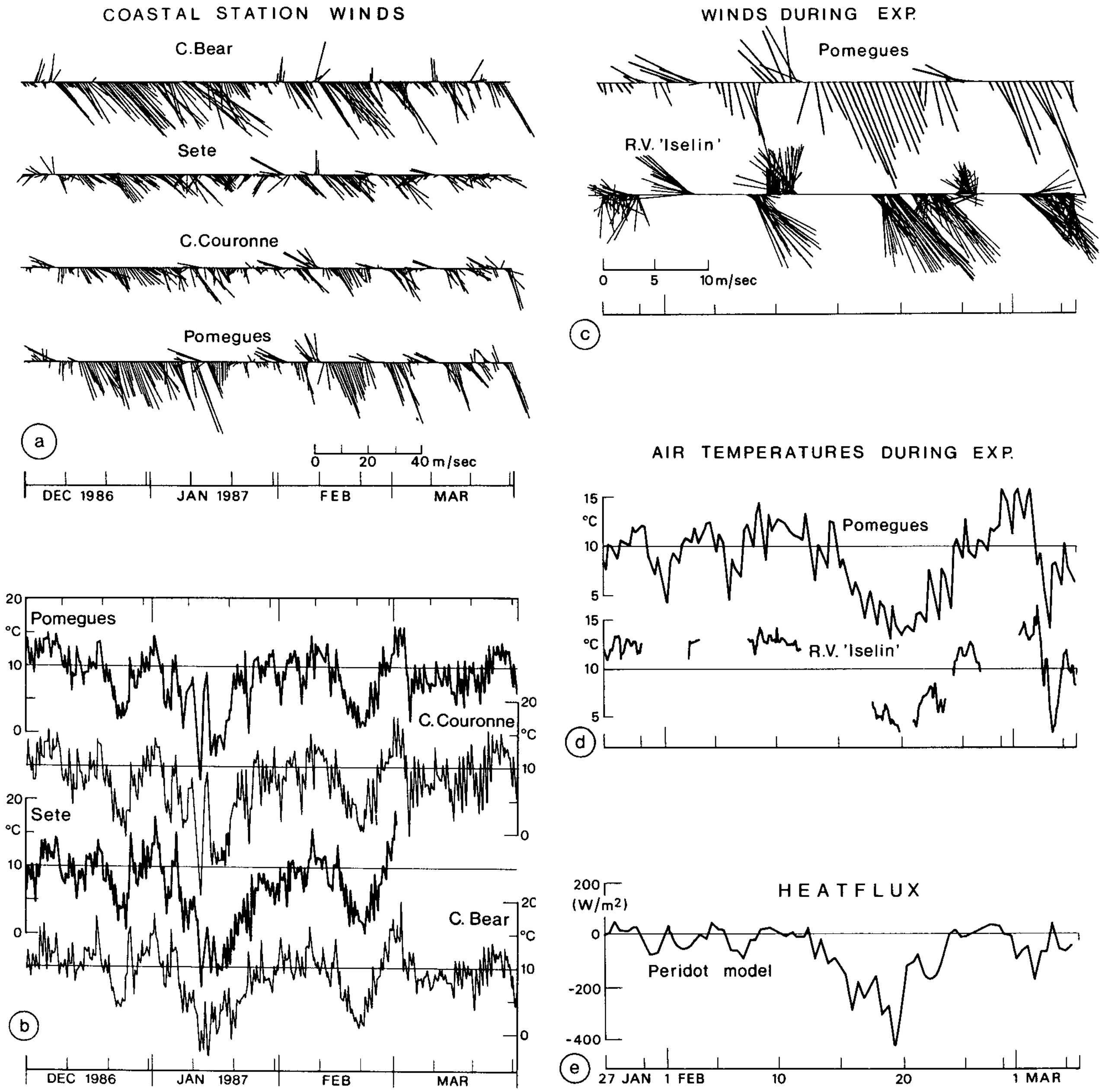

FIG. 2. (a) Vector plots of winds (direction: towards) at coastal stations (Fig. 1a) around Golfe du Lion during 1 December 1986–7 March 1987. (b) Same as (a) except for air temperatures. (c) Winds during 23 January–5 March 1987 at station Pomegues (top); and winds recorded by R/V *Iselin*, when within 100 km of the array (bottom). (d) Same as (c), except for air temperatures. (e) Total heat flux, for a grid point near the observational site in the French PERIDOT model (from Leaman and Schott 1989).

northward (Fig. 3a) in the following week of calm weather (Fig. 2c). During the next survey, 7–12 February, the patch had shrunk drastically with a wedge of stratified water penetrating from the east to near the moorings (Fig. 3b); then followed the Mistral of mid-February and a large deep-mixed area redeveloped (Fig. 3c).

In summary, the hydrographic observations of LS show that the moorings were initially deployed, during 25–27 January, in the deep-mixed regime. However, during the subsequent calm weather period stratified water was advected in, apparently closing over the patch. Later, the patch was reopened by the Mistral occurring on 15 February. From the moored array we have some evidence on the hydrographic variability through the time series of temperature fluctuations recorded by the current meters, which are discussed below. From these it appears that during the shrinking

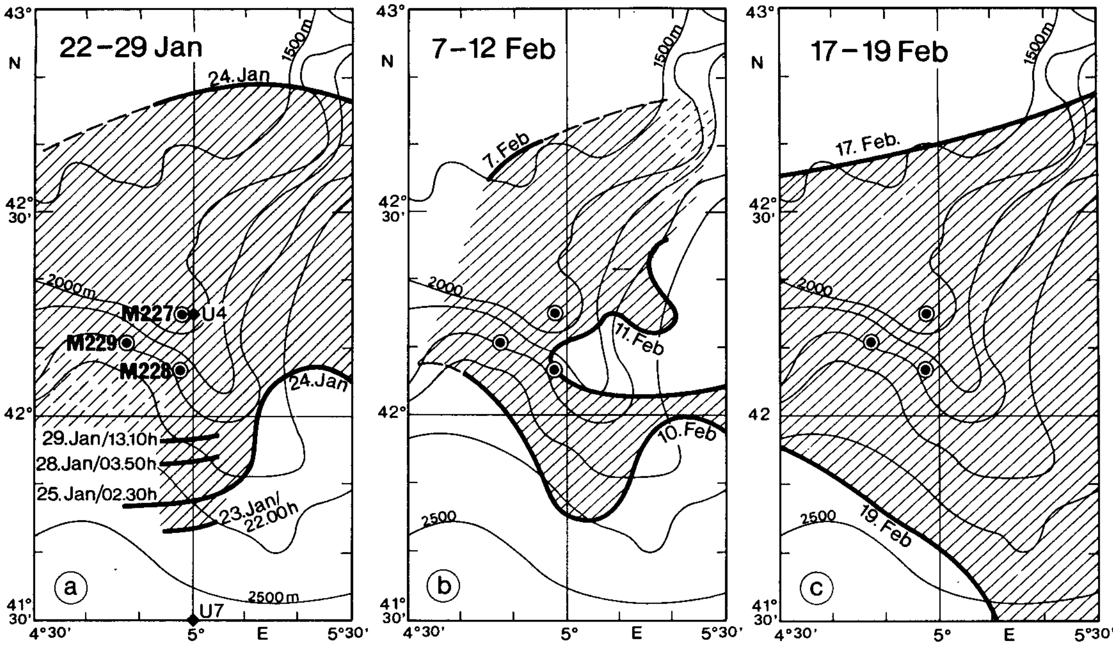

FIG. 3. Extent of deep-mixed patch during *Iselin* surveys of (a) 23–29 January (also shown are positions of CTD stations 20 and 23), (b) 7–12 February, and (c) 17–23 February 1987.

phase of the patch in early February the moorings continued to remain in homogeneous water.

3. The observations

a. Measurements of rotor currents and temperatures

The three moorings M227–M229 carried, besides the ADCPs, also conventional current meters (Fig. 1b). For comparison with the ADCP, an Aanderaa current meter (ACM) was deployed directly underneath the 150 kHz unit on M229; each of the three stations had a VACM instrument at the 1000 m level; and three more VACMs were distributed throughout the array at 1400 m, 1700 m and 2000 m.

The vertical profile of horizontal currents, judged from the rotor current measurements at station M229 in 555 m, 1020 m and 2020 m depth (Fig. 5a) is fairly homogeneous, in particular, during and after the Mistral of mid-February. In general this also agreed with PEGASUS measurements made during the same time (LS). However, on the horizontal scale of 15 km of our mooring triangle, significant horizontal shears are observed at the 1020 m level (Fig. 5b). The intense mesoscale variability with dominantly barotropic structure and small horizontal correlation scale is typical for the homogeneous winter stratification (Taupier-Letage and Millot 1986).

The overall mean currents at stations M228, M229 are about 6 cm s^{-1} to the WNW at all depths, slightly upward against the topography (Fig. 5c), while at M227, on the top of the Rhone fan, the current is only 2 cm s^{-1}; where it has to be noted, that the standard deviations of these means are of order 5 cm s^{-1}.

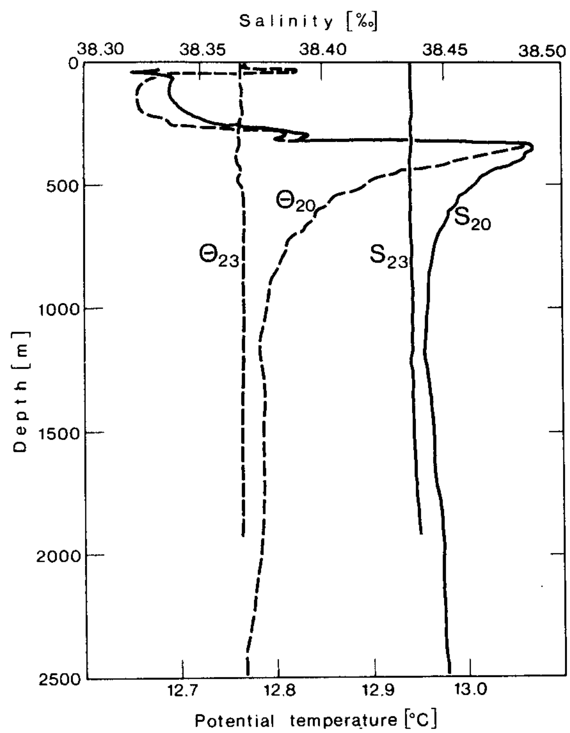

FIG. 4. Profiles of potential temperature and salinity at stations U7 (Cast 20) and U4 (Cast 23), (Fig. 3a) on 23/24 January 1987.

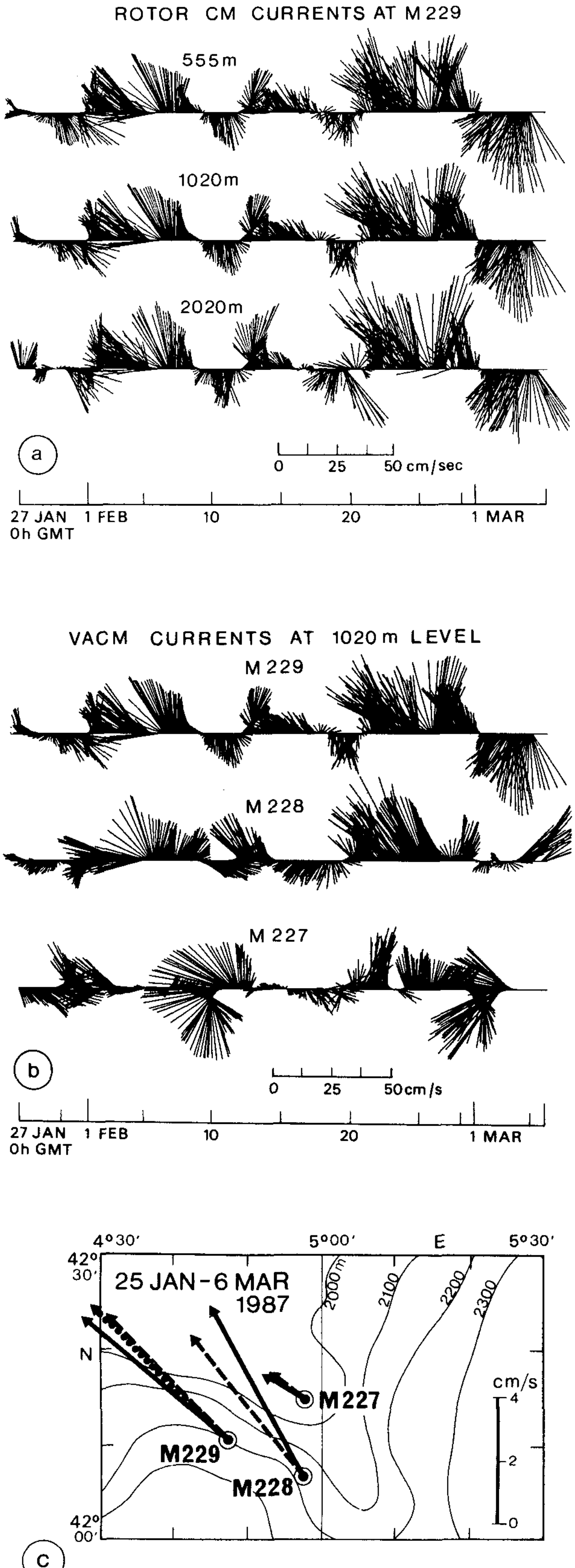

FIG. 5. (a) Forty-hour low-passed vector plots of horizontal currents at position 229, depths 555 m, 1020 m and 2020 m (water depth 2121 m). (b) Same as (a), but for the 1020 m level at positions 227, 228 and 229 (Fig. 1a). (c) Mean currents in three depth ranges during observation period.

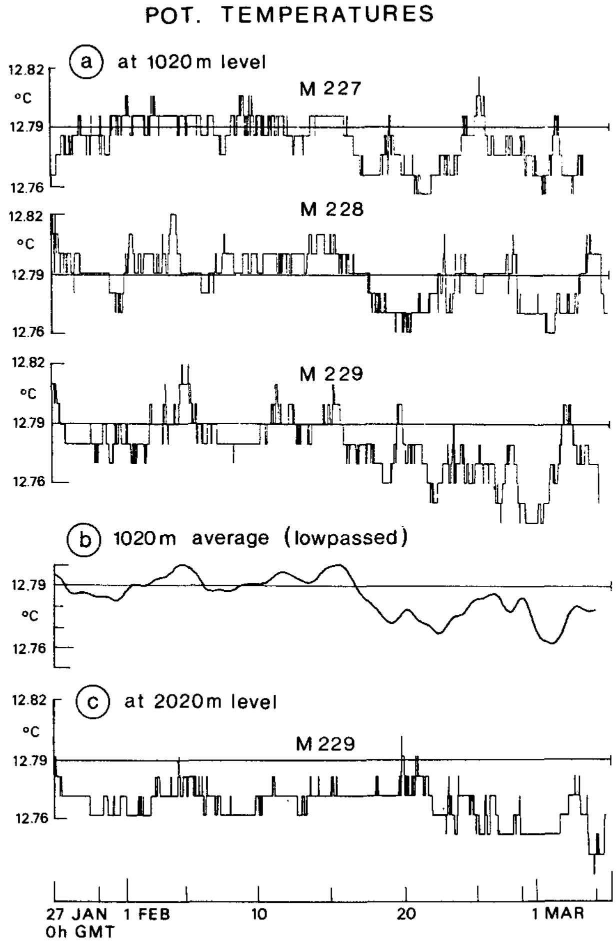

FIG. 6. Potential temperatures (a) at 1020 m level, positions 227, 228 and 229; (b) low-passed average of 1020 m records; and (c) at 2020 m level, position 229.

VACM temperatures for the same instrument combinations as in Fig. 5b are shown in Fig. 6a for the 1020 m level. As far as possible these have been corrected for compressibility, using pressure sensors to compensate for mooring motion where significant. It had been hoped that, in case the moorings had already been in place during the preconditioning phase, the temperature measurements with the accuracy available could have helped to trace the occurrence of initial deep convection, i.e., the change from profile 20 to 23 in Fig. 4, and thus provide independent evidence to compare with the direct vertical velocity measurements by the ADCPs. However, since the initial deep mixing had already taken place, the subsequent small temperature fluctuations were not adequately resolved by the VACM temperature sensors.

During early February, the deep-mixed patch shrank, and a CTD profile taken in the center of the mooring triangle on 8 February showed a similar structure as cast 20 (Fig. 4); but with the variations restricted to the depth range above about 500 m. Consequently, this intrusion of the stratified regime toward and possibly over the moorings was not detected by the uppermost temperature sensors at 555 m on M229 (ACM thermistor) and 770 m on M228 (ADCP thermistor).

The VACM temperature records from the 1020 m levels of the three stations suggest a temperature decrease beginning at about the time of the Mistral onset, around 15/16 February, which is persistent and exceeds the fluctuations and instrument noise of the preceding part of the record. When the three records are averaged and low-passed (Fig. 6b), this temperature decrease is found to be about 0.02°C, in agreement with the CTD measurements discussed in LS. At the deepest level, (the 2020 m record of station M228) a temperature decrease does not appear to occur until several days later, around 21 February, in agreement with the potential temperature time series of the CTD measurements in the 1850–2050 db layer displayed in LS.

b. ADCP data retrieval

Two ADCPs operating at 150 kHz with 20° transducer beam angle and one working at 75 kHz and 30° beam angle were used in the experiment (Fig. 1b). Parameters used were nominal 8 m bin length at 75 kHz and 8.7 m at 150 kHz (because that system's software processed the 20° beam angle data as if they were from a 30° beam angle instrument). For each acoustical signal sent (ping) the system decomposes the four received beam Doppler frequency shifts into geographical coordinates using flux-gate compass and two-axis tilt meter. 400 pings were then vector-averaged for an ensemble. With the empirical formula given by the manufacturer, this results in acoustic noise level amplitudes of the ensemble averages at 150 kHz of 0.3 cm s^{-1} for the vertical component and 0.9 cm s^{-1} for the horizontal component. At 75 kHz the noise amplitude along the beam is doubled and projected differently onto the geographical axes due to the beam angle of 30° rather than 20°, resulting in 0.7 cm s^{-1} for the vertical and 1.3 cm s^{-1} for the horizontal component. An ensemble was only stored when more than 40 pings returned acceptable Doppler data, where "acceptable" meant 3 dB above the noise level. Due to the then limited data storage capability (2 Mbyte) the ensemble time intervals selected were 1 h for M229 and M228; and 30 min for M227 (where the tape would have run out just prior to the end of the experiment).

The 150 kHz profiler at station 229 returned clean data except for a gap on 6/7 Feb (Fig. 10). The 75 kHz profiler on M228 returned a full record but during processing it turned out that offsets occurred in the Doppler data of every third bin; this effect could not be reproduced when the instrument was subsequently returned to the manufacturer. The horizontal currents of that instrument (Fig. 11a) look reasonable in comparison with the rotor current meter below it, at 1020 m (Fig. 5b); apart from a couple of dubious spikes (e.g., on 9 February), but the vertical component of that ADCP shows apparently fictitious trends of up to several centimeters per second. These were later explained by the manufacturer as being due to improper grounding of the transducers.

During the deployment phase, while preparing the ADCPs for M228, M229 and with station M227 already in the water, it turned out that due to a software change by the manufacturer the processors did not work reliably with the same parameter combinations that had been used prior to the change. Station M227 was then released for inspection after two days in the water, was found to record perfectly, and was redeployed. At the end, unfortunately, it turned out that from the redeployment only zero Doppler currents were recorded. As determined later this was due to a piece of loose solder that fell on some contacts during redeployment.

In the following we discuss the instrument behavior, including effects of mooring motion—as seen by the attitude sensors, profiles of echo amplitude, and the profiles and time series of the horizontal and vertical velocities.

4. ADCP profile evaluation and intercomparison

For each of the 400 pings used per ensemble, the along-beam Doppler shifts are projected onto earth coordinates using the beam geometry, direction from a flux-gate compass and tilt in the direction of the two orthogonal beam pairs from a two-axis tilt sensor. The overdetermination of four beams versus three coordinates allows the calculation of a so-called error velocity; this is the difference of the vertical velocity, calculated separately from the two orthogonal beam pairs. For details on the bin length calculation and echo amplitude evaluation of this experiment, we refer to Schott (1989); the actual vertical bin length, based on the sound speed in the area, was determined to be 8.2 m for the 75 kHz system and 8.9 m for the 150 kHz ADCP.

The mean beam echo amplitude at 150 kHz levels off toward a noise background of 20 dB near bin 30 or about 270 m distance from the ADCP (Fig. 7a). Simultaneously, the percentage of data stored (where "% good" means that the default value of 3 dB is exceeded) drops below 100%, as indicated by the graph on the right hand side.

At the 75 kHz system on M228 the echo amplitude levels off toward a noise background of 8 dB near bin 50, or about 420 m distance (Fig. 7b), and the per-

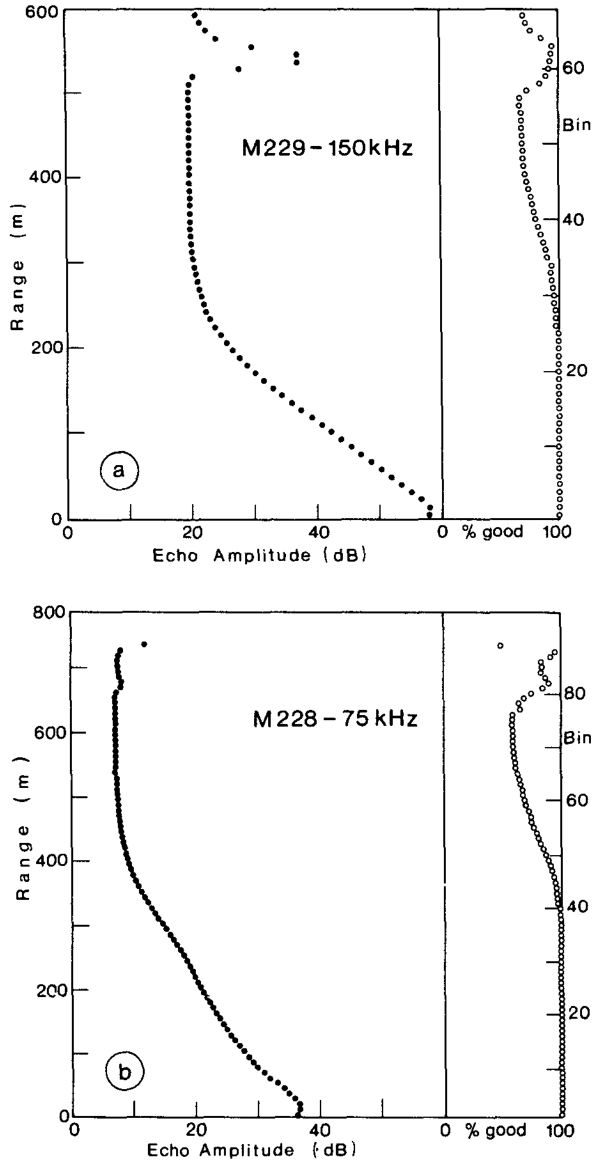

FIG. 7. Mean echo amplitude profiles and percent good data of (a) 150 kHz profile at M229 and (b) 75 kHz profile at M228.

centage of accepted data begins to decrease simultaneously. Inspection of the current profiles suggested, that biases begin to occur already at higher signal/noise (S/N) values than the default value used at that time. Chereskin et al. (1981) and RD Instruments (1989) discussed the effects of skew errors and noise bias in the different ADCP filters. The observed profile changes at low S/N in our measurements are due to the admixture of noise to the Doppler signal. In order to be on the safe side, we limit the data presentation in most of the following to the lower part of profiles where S/N > 10. At 150 kHz this is the case for bin 20 or a range of about 180 m and at 75 kHz for bin 32 or about 260 m range.

The instrument behavior of the 150 kHz ADCP on station M229 during the deployment period is apparent from Fig. 8. The depth of the ACM under the 150 kHz system on M229 shows long periods of almost no mooring motion (Fig. 8a), particularly during the Mistral period of 15–22 February, but excursions exceeding 100 m were observed during the barotropic current events occurring after 22 February (Fig. 5a). Tilt of the instrument axis mostly does not exceed 1° and is less than 3° even in the strong current event at the end (Fig. 8a). Ensemble mean instrument orientation, i.e., rotation around the vertical axis changed, in general, only gradually throughout the experiment. Standard deviations of orientation and the two tilt measurements were also stored for each 400 ping ensemble. For the tilt measurements it did not exceed ± 0.1°, and for orientation it was small during most of the experiment. However, noticeable instrument axis rotation occurs during the Mistral of 15–22 February. In summary, the 150 kHz system on M229 was pointing almost straight upwards during the entire experiment, and did not show anomalous behavior during the Mistral, except for some increased rotation around

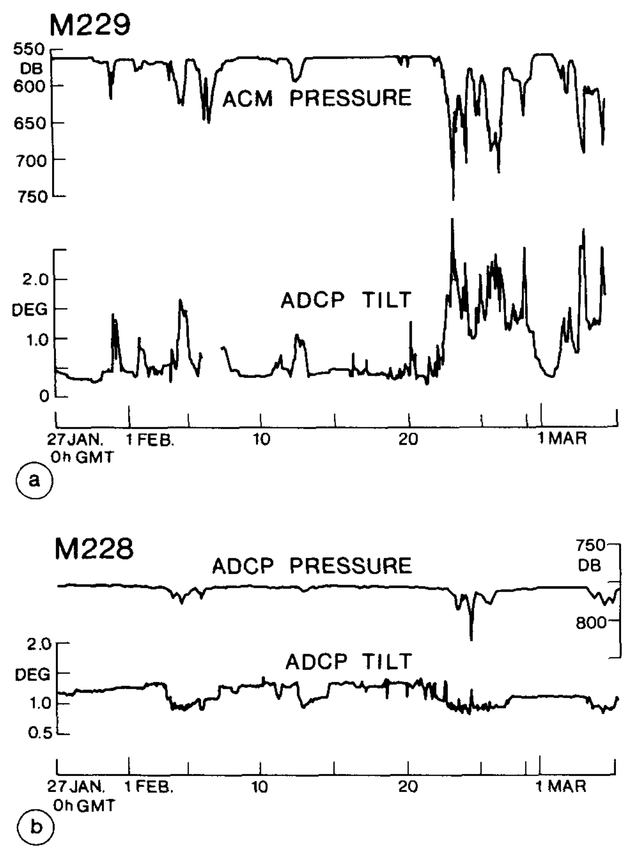

FIG. 8. (a) Attitude sensors of the 150 kHz profiler on M229: pressure (recorded by ACM underneath the ADCP; top) inclination (bottom). (b) Same as (a), but for 75 kHz profiler on M228 where pressure is internally recorded by ADCP.

the axis, possibly due to the effects of the vertical currents past it.

The 75 kHz system (on M228), due to more buoyancy of the top float, did not show the significant depth excursions of the 150 kHz during the barotropic current events; and its tilt varied only in the range of 0.3° to 1.3° (Fig. 8b).

The analysis of all the data showed that there were also biases in the Doppler data of the first bin, not noticeable in the horizontal currents but only in the vertical component, which are due to reverberation effects reaching up into the first bin, beyond the blanking range of 2 m that we had selected.

Comparison of the horizontal currents measured acoustically by the 150 kHz system of M229 in bin 2 (centered at 537 m) with those measured by a conventional ACM rotor instrument is shown in Fig. 9. There is an almost perfect agreement of both current components, with correlation coefficients of 0.97 for the one-hourly u-components and 0.98 for the v-components. This good agreement is helpful for our subsequent discussion of the vertical currents.

For small differences in the short-period fluctuations one has to remember that the ACM, because of its large current vane, has response problems for periods shorter than about two hours (e.g., UNESCO 1975).

5. Time series of the doppler current measurements

Time series of unfiltered horizontal current vectors for bins 2, 10, and 20 ranging from 537 to 376 m depth are shown in Fig. 10a for the 150 kHz ADCP profile of M229. In the deeper current measurements of this station (Fig. 5b) a strong vertically homogeneous northward flow appeared during 22 February–1 March, reversing to southward for the remainder of the recording period. The acoustically measured currents show that this current appears to reach all the way up to near the surface (Fig. 10a).

The measurements of interest to us, for which the experiment was carried out in the first place are, of course, time series of the vertical currents. These are

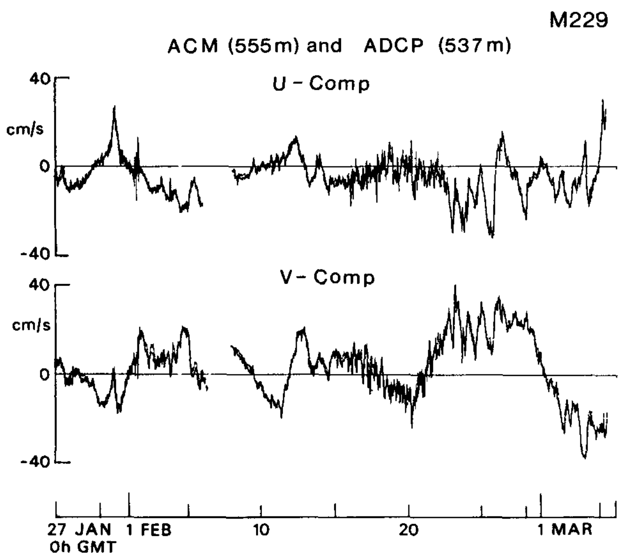

FIG. 9. Comparison of east (u) component (top) and north (v) component (bottom) of ACM rotor current measurements (at 555 m) with acoustic Doppler current measurement at bin 2 (depth 537 m) of 150 kHz profiler on mooring M229. They are almost identical.

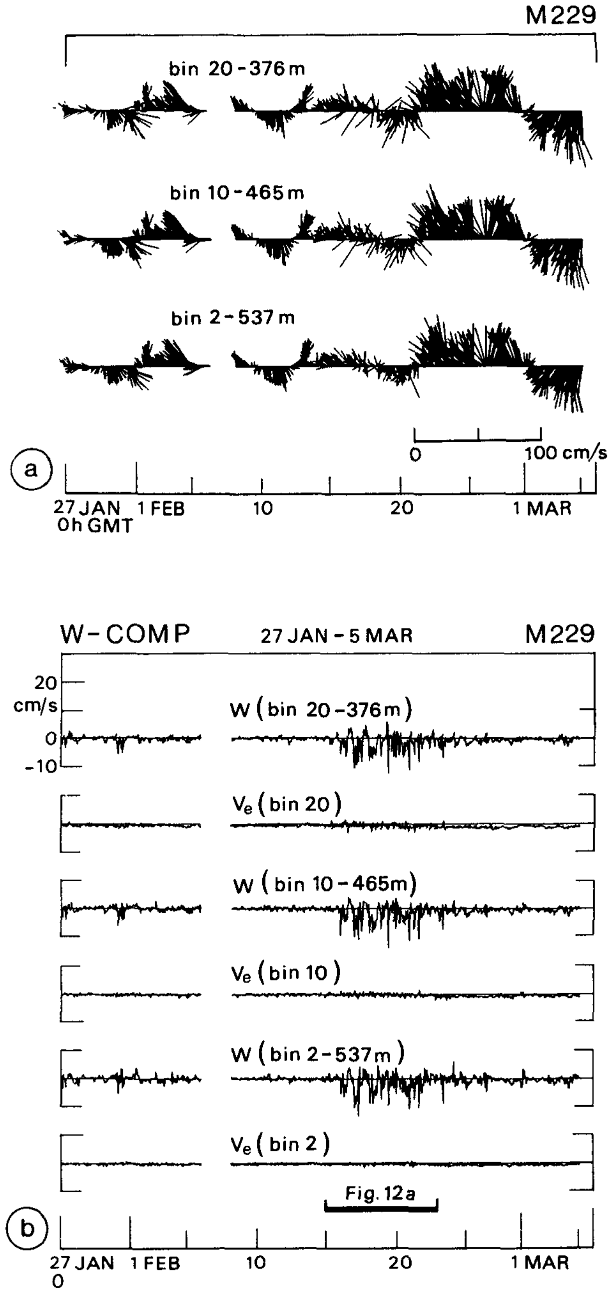

FIG. 10. (a) Horizontal current vectors recorded by 150 kHz ADCP on M229 during 22 January–5 March, for bins 2, 10 and 20. (b) Same as (a) but for vertical velocity components, w, and error velocity, v_e (definition see text); Mistral week is marked by heavy bar.

shown in Fig. 10b for bins 2, 10, and 20, i.e., from 537 m, 465 m and 376 m depth. Also shown, for the three bins, are the error velocities. As already mentioned, while the vertical component is the average of the vertical projection of all four beams, the error velocity is the difference of vertical velocity calculated from both beam pairs independently. It thus provides an indication of the consistency of the signal among the beams. Also marked is the period 15–22 February, during which the Mistral event occurred (Fig. 2). While vertical velocities are small in the quiet period prior to the Mistral, strong downward velocities occur during the Mistral with weaker upward motion in between. These downward velocities seem to be vertically coherent over at least 200 meters. These motions appear to be real, because of two factors: First, they exceed by far the error amplitudes which during this time period do not differ much from those of the quiet period (Fig. 10b); and second, they have the same magnitude as the horizontal currents which do not show anomalous behavior in comparison with the rotor current measurements (Fig. 9).

One possibility that the signal might be real but still not representing real water motion is that of vertical scatterer migration through the water. such scatterers could be zooplankton or particles carried seaward by the offshore Mistral winds. A typical period of active vertical scatterer motion is the diurnal cycle where zooplankton migrates upward after sunset and downward after sunrise. This effect, which shows up as a spectral peak both in echo amplitude and vertical velocity and as significant coherence between these two parameters, was reported from earlier near-surface ADCP measurements (Schott and Johns 1987; Johns 1988). In our case, the echo amplitudes and vertical velocities do in fact show peaks and coherence at the 24-hour period, but the important fact is that in the period range of several hours of the convection events significant coherence between both parameters does not occur.

There is an apparent mean vertical current of about -0.3 cm s^{-1} during the time of no vertical velocity currents; this is a bias typical for the ADCPs we used, and we have to consider any convection related velocities relative to this bias.

The vertical currents of the 75 kHz profiler, presented in Fig. 11b for bins 2, 15, and 30 from the depth range 757–527 m show variations over periods of days that are also reflected in the error velocities and therefore spurious; they are related to the hardware problem described above. Nevertheless, there is enhanced short-period variance during the Mistral period also in these ADCP data. In the further analysis we will concentrate on the 150 kHz system of M229 and use the 75 kHz data only for comparison. In particular, we will investigate in some detail the Mistral period of 15–22 February and compare it with the quiet week of 8–15 February preceding it.

The vertical currents of Figs. 10b, 11b are shown expanded in Fig. 12, for the time period 15–22 February. We now see more clearly one disadvantage in our data recording, which stored ensembles only every hour in the ADCPs on M229 and M228, due to the limited tape capacity (the ADCP on M227 which stored at 30 min intervals, did not work): the downward events, in many cases, are only supported by single ensembles. Apparently a 15 minute or even shorter ensemble time interval would have been required to better document the downward events. Yet, as discussed above, the vertical velocities are significant and appear to be real signals.

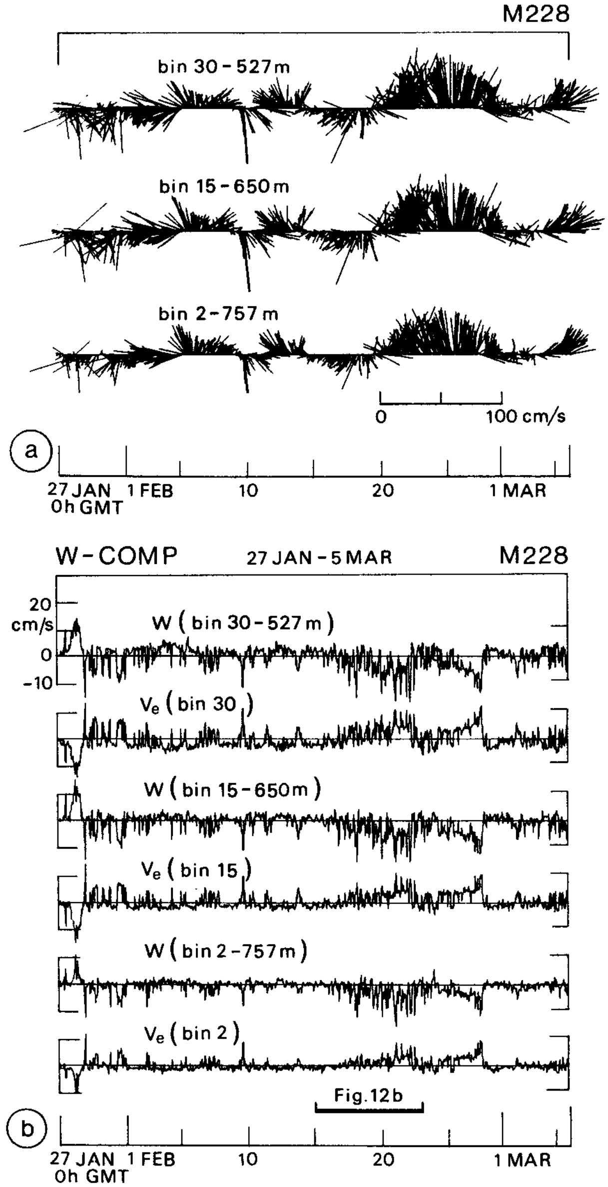

FIG. 11. (a) Same as Fig. 10a, but for 75 kHz ADCP on M228 and bins 2, 15, 30; (b) same as Fig. 10b, but for M228.

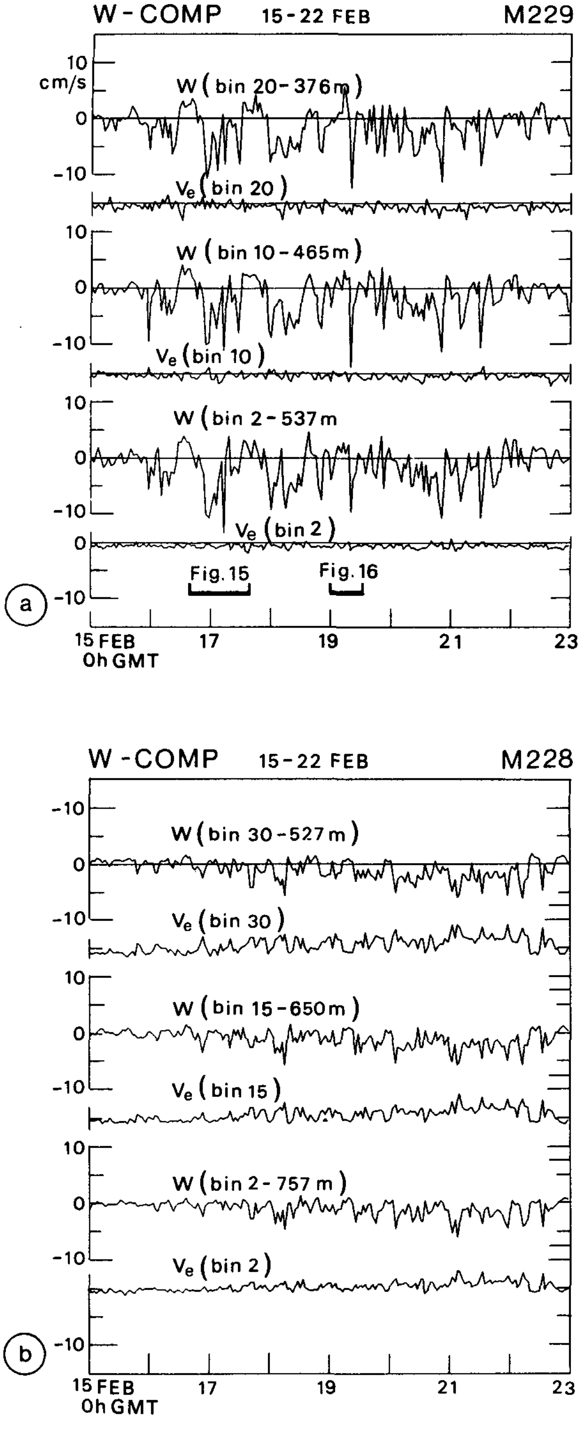

FIG. 12. (a) Vertical velocities and error velocities recorded in bins 2, 10 and 20 of 150 kHz ADCP on M229 during the Mistral period 15–22 February. (b) same as (a), but for 75 kHz ADCP on M228 and bins 2, 15, 30.

Before inspecting some events, in particular the period 16/17 February in more detail, we compare the Mistral period velocities statistically with those of the quiet period preceding it.

6. Velocity and temperature fluctuations during the mistral week

The mean vertical velocity measured by the 150 kHz ADCP on M229 during the Mistral week, 15–22 February, and averaged over the first 20 bins of apparently good data quality, is -1.6 cm s^{-1}, compared to -0.3 cm s^{-1} in the preceding week, while the error velocity stayed the same, at -0.6 cm s^{-1} (Table 1). This mean downward motion was apparently due to the larger downward than upward velocity event averages (Fig. 12a). When judging this result for the mean speed it has to be kept in mind, first, that the sampling is not adequate to resolve the short-period downward bursts; this should in fact cause a positive (upward) bias. And second, that the weaker upward velocities in between the downward events are not large compared to the ensemble noise amplitude and the error velocity.

For the 75 kHz ADCP, the mean velocity difference for the Mistral week against the pre-Mistral week is -2.6 cm s^{-1} but the error velocity changed by about the same amount (Fig. 12b, Table 1).

High-frequency variance in the horizontal currents occurs at all depths after the onset of the mid-February Mistral. This is already apparent upon inspection of the unfiltered ADCP/ACM comparison records of Fig. 9, but becomes very obvious after high-pass filtering the currents with 6-hour cutoff period; as shown in Fig. 13a for the u-components of various depth levels (v-components look similar). The top two records are the ADCP currents (bin 2) of the 75 kHz system on M228, and of the 150 kHz system on M229; the third record is the ACM underneath the M229 150 kHz profiler and at deeper levels all records are from VACMs.

The onset of energetic fluctuations occurs with distinct differences in time, as Fig. 13a and more clearly a plot of HF kinetic energy (Fig. 13b) shows. They begin first about 0600 UTC 16 February at 550 m and 1020 m of station M229 and at 1020 m of M228, about half a day later at 1020 m and 1420 m of station M227, and almost two days later at about 2200 UTC 17 February at the two deepest levels, 1720 m at station M228 and 2020 m at M229.

Unfortunately the temperature records are too noisy to clearly determine the onset times of cooling at the different levels after the start of Mistral-related surface heat loss. At the 1000 m level, temperature decreases are detected at about the time of high frequency (HF) fluctuation onset (Figs. 6a,b) during the morning of 16 February.

At the deepest level, there is apparently first a slight warming (Fig. 6c) after the HF fluctuations have already begun; cooling to below the temperature level of the preceding week does not occur until late 21 February, about 4 days later. But horizontal currents at that level change drastically during that time (Fig. 5a) suggesting the possibility of advection of different water mass properties.

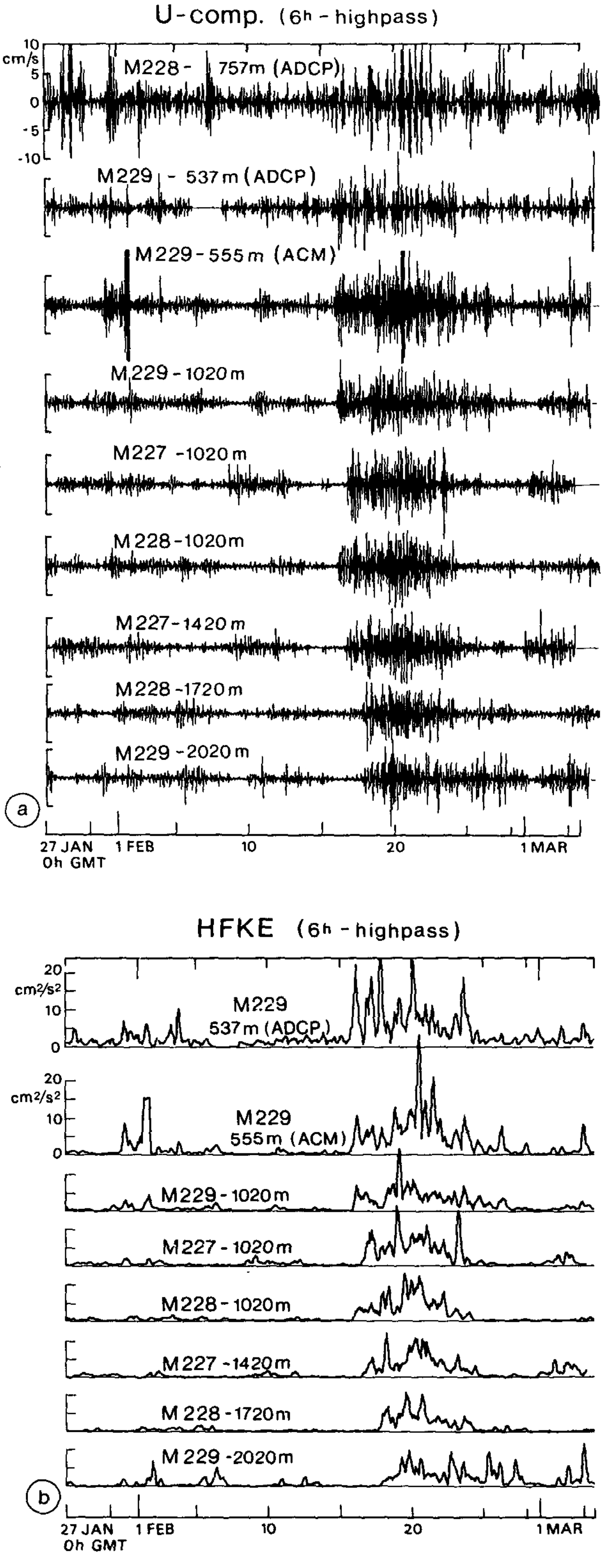

FIG. 13. (a) High-passed current fluctuations (periods longer than 6 hours eliminated) for current records between 537 and 2020 m depth. East component only is shown (north component qualitatively similar). (b) Horizontal fluctuative kinetic energy (HFKE), calculated for sliding 6 hour segments of 6 hour high-passed currents.

LS shows the averaged temperatures for the depth ranges 1850–2050 db from CTD casts taken in the vicinity of the moorings (their Fig. 17). On 18 February two casts still show approximately pre-Mistral temperatures; while two casts taken on 21 February show a decrease by about 0.015°C. This suggests that the onset of HF fluctuations at depth leads the onset of cooling by several days. It should be noted that the cooling in the CTD profiles of LS is associated with a compensating salinity increase, i.e., no density increase occurs during 18–24 February at the deep levels.

7. Variances and spectra

Averages of vertical and horizontal kinetic energies of the ADCP records for 20 bins in the range where the acoustic data quality was supposedly good (Fig. 7) are shown in Table 1, both for the original one-hourly data and again after application of the 6-hour high-pass filter. The horizontal kinetic energy of the unfiltered data is mostly associated with the background flow and does not vary that much from the pre-Mistral to the Mistral week (Fig. 5a,b). Vertical kinetic energy of the 150 kHz profile is 10.2 cm^2 s^{-2} during the Mistral week compared to 0.3 cm^2 s^{-2} for the preceding week. After applying the 6-hour high-pass filter, these values are 3.7 and 0.1 cm^2 s^{-2}, respectively—both to be compared with an error velocity variance of 0.1 and 0.2 cm^2 s^{-2}, respectively. The vertical kinetic energy measured by the 75 kHz system for the Mistral week is similar (5.3 cm^2 s^{-2}), but the error amplitude is much larger (2 cm^2 s^{-2}) than for the 150 kHz profile.

The high-pass filtered horizontal fluctuating kinetic energy (HFKE) measured by the ADCPs during the Mistral, i.e., that associated mostly with the downward events compares to the vertical KE approximately as 4:1 in both measurements (Table 1). At the 1000 m level, the HFKE, averaged over the three records from stations 227, 228 and 229, is 4.1 cm^2 s^{-2} during the Mistral week, compared to 0.4 cm^2 s^{-2} for the pre-Mistral week (Table 2). This tenfold energy increase agrees with that observed by the 150 kHz ADCP (Table 1); but the energy level of that measurement in the range 376–537 m depth was a factor of three higher than for the 1020 m VACM measurement. Part of this energy increase toward the surface can be real, part of it will be due to aliasing by the 1-hour sampling rate of the ADCP. At the levels below 1000 m the energies during the Mistral week decrease further, but partially due to the delayed response (Fig. 13).

The slope of energy energy density spectra of horizontal kinetic energies (Fig. 14) decreases for the Mistral week against the preceding week. The nearly linear drop-off for the VACM records at the 1020 m level is −2.8 during 8–15 February and −1.2 during 15–22 February (Fig. 14a). At the 555 m level ACM on M229 the slopes are similar, −3.3 versus −1.2. For the ADCP currents, the spectra are not as linear as for the rotor

TABLE 1. Means and variances (over depth ranges) of ADCP currents during 8–15 February (quiet period) and 15–22 February (Mistral period)

Profiler	Time segment	High-pass filter applied?	Means $\bar{u}$	$\bar{v}$ (cm s^{-1})	$\bar{w}$	$\bar{v}_e$	Variances $\overline{\frac{u'^2+v'^2}{2}}$	$\overline{w'^2}$ (cm^2 s^{-2})	$\overline{v_e'^2}$
150 kHz/M229	2/08–2/15	*n*	0.1	2.0	−0.3	−0.6	60.3	0.3	0.1
(bins 2–20; 537–376 m)		*y*					1.3	0.1	0.1
	2/15–2/22	*n*	−4.2	2.2	−1.6	−0.6	74.1	10.2	0.4
		y					13.0	3.7	0.2
75 kHz/M228	2/08–2/15	*n*	0.9	2.9	0.2	−0.7	95.0	4.9	3.9
(bins 8–27; 707–552 m)		*y*					6.9	1.2	0.9
	2/15–2/22	*n*	−0.4	3.4	−2.5	1.3	181.8	16.3	8.4
		y					22.4	5.3	2.1

currents; visually estimated linear slopes yield −1.8 to −2.4 for 8–15 February and about −0.9 to −1.2 for 15–22 February (where one has to note the different energy scales of the graphs of Fig. 14 and the larger confidence bars on the ADCP spectra than on those of the averaged spectra for the three VACM records). The vertical current spectrum (Fig. 14d) falls off at about −0.6 during the Mistral week and is mostly just noise for the preceding week.

Cross-spectra for the vertical velocities show high coherence and insignificant phase change over the entire range, as to be expected after inspection of the time series (Fig. 12). Here the question is how real is this vertical homogeneity and how much of it has to do with the bin-to-bin tracking of signals.

The recorded temperature fluctuations are not helpful for analyzing the shorter-period variations; we could barely resolve the general decrease by 0.02°C after the Mistral onset (Fig. 6), but the HF variances for the two week-long periods are the same, i.e. they are dominated by instrument noise.

8. Inspection of individual events

A possible assumption is that the vertical velocity events are associated with some kind of a three-dimensional circulation feature—maybe a small vortex—that is advected past the observation site by the background mean flow. In order to judge how mean flow and event current might superimpose in such a scenario, inspection of individual events is necessary.

During the 24-hour period 1600 UTC 16 February–1600 UTC 17 February, four events exceeding 5 cm s^{-1} downward velocity occurred (Fig. 15a). Events appeared to be simultaneous over the range of good data retrieval (here we extend the graphs up to bin 30 for comparison), and they by far exceed the error amplitude (Fig. 15b). In particular, the error amplitude has no organized pattern correlated with the downward velocity pattern. Similarly, the individual beam-echo amplitude plots do not show a systematic relation with the downward velocities. Instrument depth remained constant during this 24-hour period.

A clearly detectable horizontal current anomaly is only associated with the first event, 2200–2300 UTC, and it seems to be restricted to bins above 10 (Fig. 15c). The background current around the time of the event is to the NNW. At 2200 UTC, the current vector points toward NW and at 2300 UTC toward SW. Prior to the onset of strong vertical motion, the current backs from NNW to W. A clockwise spinning vortex, advected past the observation point by a northwestward weak mean flow and cut by the ADCP mooring near its center would first cause a deflection of the current vector toward the north (2200 UTC) then toward the SW (2300 UTC), as observed. An anticlockwise eddy would better explain the westward deflection prior to the onset of vertical motion (2100 UTC) but would not explain the southwestward orientation at the end (2300 UTC). During the other three events, current variation is not marked enough to speculate on any association with vortex motion.

The event on 19 February exceeds 10 cm s^{-1} over much of the range (Fig. 16a), while error velocities were less than 1 cm s^{-1}. Pressure indicates that the instrument stayed at a constant level during the event.

TABLE 2. 6-hourly high-passed fluctuative kinetic energy measured by VACMs

Instrument	Depth (m)	8–15 February (cm^2 s^{-2})	15–22 February (cm^2 s^{-2})
22702	1020	.53	4.37
22802	1020	.20	4.19
22903	1020	.56	3.71
mean at 1020 m level		.42	4.09
22703	1420	.41	3.52
22803	1720	.18	2.74
22904	2020	.43	2.22

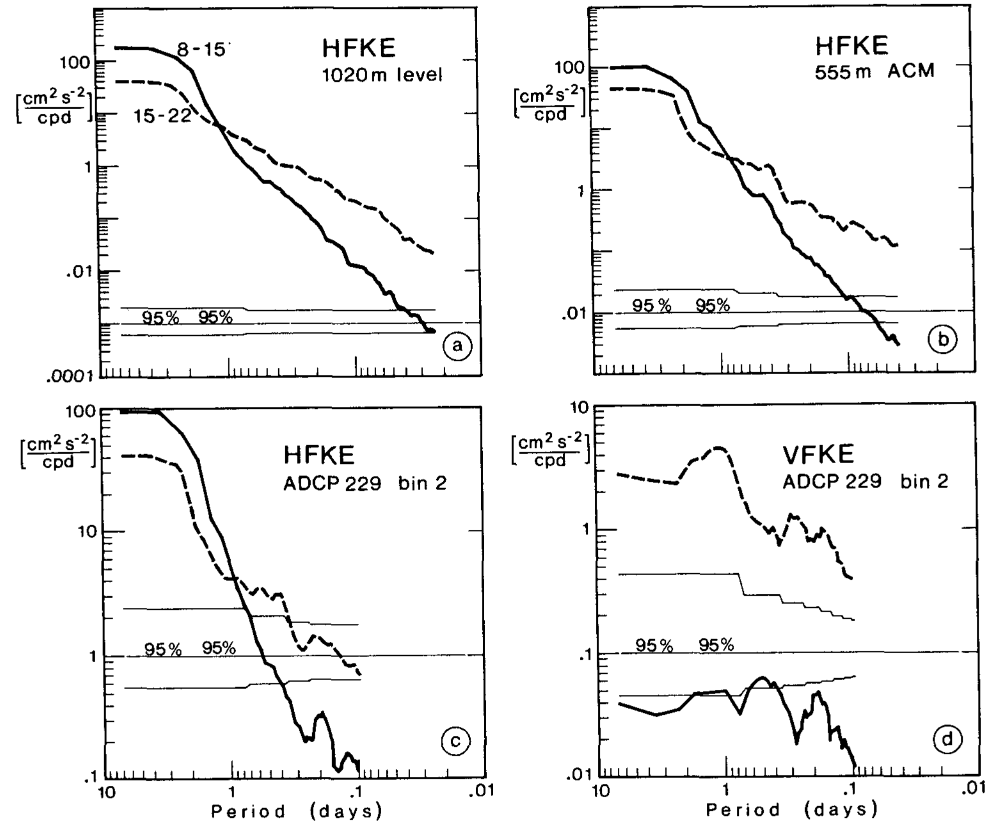

FIG. 14. Energy density spectra (a) of horizontal fluctuative kinetic energy (HFKE) at 1020 m level, averaged over the 3 VACM records of M221, M228 and M229; (b) of HFKE of ACM record at 555 m, station M229; (c) of HFKE of ADCP record at 537 m of 150 kHz system on M229; and (d) same as (c) except for vertical fluctuative kinetic energy.

The horizontal currents during the event show a change from southeastward to southwestward; while prior to the event the horizontal current was weak southward (Fig. 16b). This horizontal current pattern would be consistent with a counterclockwise eddy advected past the instrument site from the north with the southward background flow. But here again one has to be cautious because these horizontal current variations at event time are not any more noticeable than in the preceding several hours. At 1020 m depth the strongest VACM current of that 12 hour period occurs between 0700 and 0800 UTC, but that could be unrelated to the vertical velocity event in the 300 to 500 m depth range.

In summary, there is no clear evidence for a typical organized pattern of horizontal currents associated with the vertical velocity events. Temperature sensors, as already stated, were not accurate enough to help with any indication of water mass changes during these events. Our vertical velocity events can not be associated with instability eddies (Gascard 1978) which are shed from the front and can drift into the interior of the patch. They would be associated with a temperature signal that should be detectable at the 600 m level by our sensors.

9. Summary and discussion

During 24 January to 5 March a triangular array of three ADCPs was moored in the Golfe du Lion, south of France on top of a topographic feature called the Rhone fan. This location has been found in the MEDOC studies of 1969–75 to be a preferred location for the occurrence of deep mixing. Unfortunately, the initial breakthrough of the near-surface pycnocline and subsequent occurrence of deep convection could not be observed in our case because an unusually early and strong Mistral occurring around 10 January had already caused a deep-mixed regime prior to the beginning of the experiment. Two of the profilers, one working at 150 kHz, looking upward from 552 m and the other one working at 75 kHz at 765 m returned a complete dataset of three-dimensional currents measured at one-hour ensemble time intervals at 8 m bin length where an ensemble consisted of 400 pings.

The vertical currents in the deep mixed regime are small during the first three weeks of moderate winds, but bursts of short-period downward motion appear during a second Mistral, which occurred during 15–22 February. These downward velocity events, which

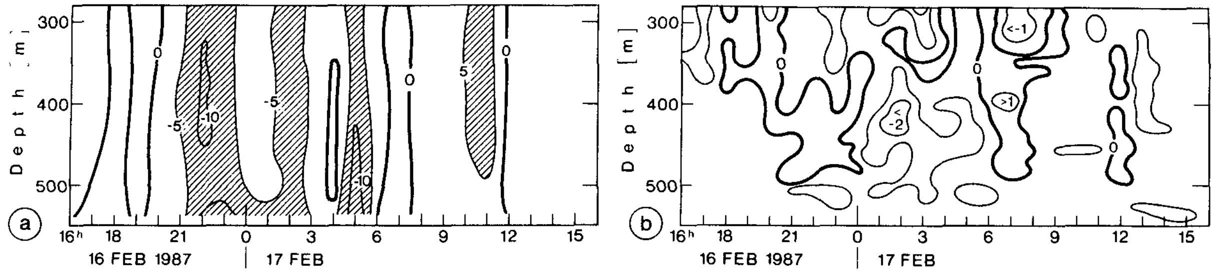

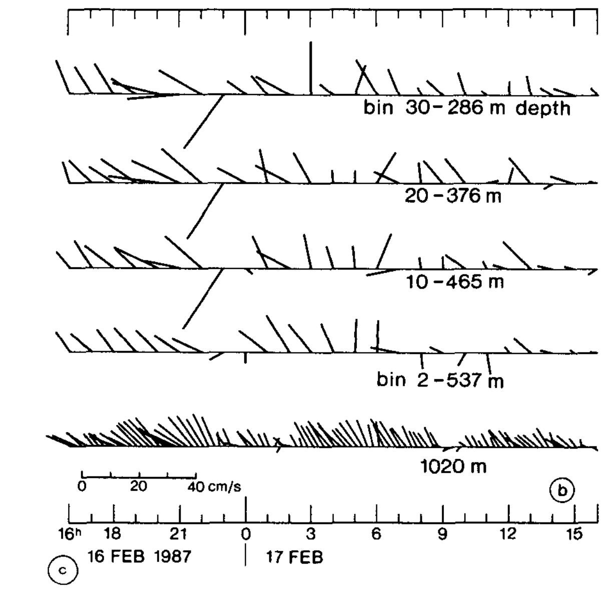

FIG. 15. (a) Time-depth contours of vertical velocity at M229 for 16 February 16:00–17 February 16:00 in depth range 290–540 m (time interval 1 hour). (b) Same as (a), but for error velocity. (c) Current vector plots of several ADCP bins during same time period; and of VACM at 1020 m (time interval 15 min, bottom).

are poorly resolved by the one-hourly ensembles, appear to be homogeneous over hundreds of meters in the vertical.

A number of tests suggest that these velocity events are real; at least for the 150 kHz ADCP on mooring 229: (i) the horizontal currents compare well with rotor current measurements underneath, confirming that the instrument worked well; (ii) no projection of the horizontal component onto the vertical axis is found [this was already tested for that same 150 kHz profiler in a previous application in the Somali Current (Schott and Johns 1987)]; (iii) instrument depth remained constant during the events, i.e., they could not have been caused by mooring motion; (iv) the "error velocity" that can be calculated due to the overdetermination of having four beam Dopplers available for three Cartesian velocity coordinates, is much lower than the vertical velocity during the events; (v) vertical motion of scatterers through the water could not have been the cause because no significant coherence with backscatter energy variations was found at the event periods. Still, in the interpretation of the profiles one needs to keep in mind that vertical structure depends on the skill of the ADCP to track variations from one bin to the next; hence part of the homogeneity in the vertical velocity events delivered by the ADCPs might be instrument-made.

The short-period vertical current fluctuations at the ADCP level are associated with horizontal current fluctuations for which no clear and persistent event structure could be derived. Short-period horizontal current fluctuations were also observed deeper down by VACM measurements. The vertical kinetic energy during the Mistral week, for periods shorter than 6 hours and averaged over the depth range 550–370 m, is 10.2 $cm^2\ s^{-2}$ compared to 0.3 $cm\ s^{-2}$ for the preceding week; and the ratio of horizontal to vertical kinetic energy is about 4. Horizontal kinetic energy spectra of the VACM currents for the quiet week preceding the Mistral fall off at about a -3 slope, while during the Mistral and convection the spectral slope is -1.2 without definite peaks at any particular period.

It does not appear that in either period the variance was due to internal waves. In particular, the vertical fluctuations during the Mistral cooling period do not look like internal waves with their asymmetry between downward and upward motion. A Brunt–Väisälä frequency can not be defined in the homogeneous water

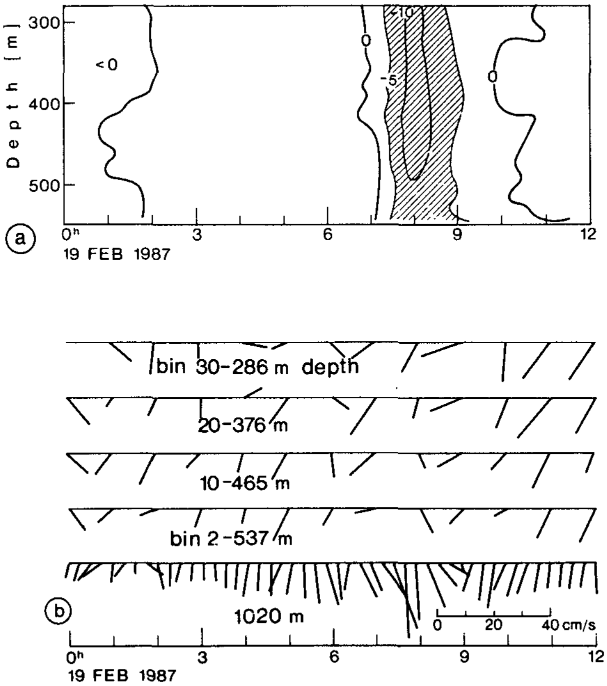

FIG. 16. (a) Time depth contours of vertical velocity at M229 for 0000–1200 UTC 19 February in depth range 200–540 m. (b) As Fig. 15c, but for 19 February.

body (for a profile see cast 23, Fig. 4) which might otherwise have been used to calculate the ratio of vertical to horizontal kinetic energy for internal waves and compare it with our observations.

The HF variability apparently needs negative heat flux. During a period of strong winds in early February high frequency energy bursts are not observed (Figs. 2, 13) although during most of this period the moorings were located in almost totally homogeneous water. Hence, mechanical wind or wave forcing, e.g., Langmuir circulation, which has been found to be associated with vertical currents of more than 10 cm s^{-1} in surface-mixed layers (Weller et al. 1985) and might be suspected to penetrate into the upper part of the ADCP range due to the lack of vertical stability, cannot be the cause of the observed HF variations. Instead, the conclusion is that the short-period fluctuations are associated with convection following surface cooling.

The interesting connection to the larger-scale hydrography was that the HF fluctuations at the 1020 m level and above occurred in conjunction with the slight cooling of the deep-mixed patch. This amounted to 0.02°C beginning 16 February, and no exact determination was possible of the timing between onset of the fluctuations, which also showed horizontal time lags between stations (Fig. 13), and cooling due to low resolution of the temperature measurements. However, at the 2000 m level the HF variability began nearly two days later, and cooling there seemed to be delayed by two more days against the onset of HF fluctuations.

In the ADCP measurements of only one-hour time resolution, no vertical phase propagation of the downward velocity events during the convection period could be detected. A possible interpretation of the events then is that they are "frozen", i.e., quasi-stationary (at the time scale of the observations) features, being advected past the observation point by the background mean current. Since the background flow is fairly homogeneous, they are not sheared apart. From the duration of the events (typically < 2 hours) and the background mean flow (typically < 20 cm s^{-1}) we can estimate that the horizontal scale of the cells has to be <1.4 km. Of course, the alternative interpretation that the events are forced in place, spinning up simultaneously over the range of ADCP, is also possible. A distinction could only be made by measuring the vertical passage of water mass properties, which was unfortunately not possible at the resolution of our temperature sensors. An indication of a similarly small horizontal scale of convection events was reported by Gascard and Clarke (1983), who analyzed the motions of rotating floats in the Labrador Sea. While one float showed intense downwelling of 9 cm s^{-1}, a second one—only about 1 km away—did not. (This could, of course, also be interpreted as one float sitting just within a larger convection region, the other one just outside of it.)

If we believe the horizontal scale as derived based on the frozen assumption, it implies that there are three different scales present in a convection regime:

1) the scale of the homogeneous patch itself, the chimney scale of some tens of kilometers (MEDOC group 1970; Killworth 1976), and probably up to O (100 km) if several chimneys merge or extended Mistral cooling expands an existing chimney;

2) the scale of the eddies detached from the front around the homogeneous patch of the scale of the Rossby radius of the stratified regime, about 5 km (Gascard 1978);

3) the convection cells of O (1 km) found here.

The lifetime of the short-period fluctuations must be less than O (1 day), because they quickly disappear when the heat loss returns to small values around 24 February (Figs. 2e, 13).

With the mean vertical velocity of −1 cm s^{-1} found during the Mistral week, one could be tempted to speculate on the deep water renewal. If the area where this occurred is of size 50 km by 50 km (Fig. 3), the downward transport would amount to 25 Sv (Sv ≡ 10^6 m^3 s^{-1}) for the one-week duration of the Mistral. If two Mistrals occur per year that would mean an annual deep water renewal rate of 1 Sv, in the right magnitude compared to what has been estimated by the temperature–salinity budget method (Bethoux 1980). Of course, there has to be upward motion elsewhere in the region and hence, we assume that the downwelling area is smaller than the total homogeneous area.

The horizontal circulation associated with deep water formation, modeled analytically (Crépon et al. 1989) or numerically (Madec et al. 1990), is cyclonic around the convection zone on top and anticyclonic on the bottom, which is basically explainable by potential vorticity conservation of a water column that is stretched at the top and compressed at the bottom. If the small convection cells in the interior of the patch feel the Coriolis force, a possible scenario (J. Marshall, personal communication) is to interpret them as point vortices, each rotating cyclonically on top and anticyclonically at depth. Their individual vorticities would add up to a large-scale cyclonic circulation around the regime on top and anticyclonic at depth. The Rossby radius in the interior could be small enough to easily permit the existence of small vorticities of O (1 km) scale, but analysis of horizontal currents during vertical velocity events does not support preferred cyclonic rotation. Further, their lifetime appears to be too short for geostrophic eddies. The mean currents measured at our three stations also do not show a baroclinicity supporting the change from cyclonic to anticyclonic circulation with depth; maybe they are too far away from the rim of the deep-mixed area.

Acknowledgments. The moored station work was carried out by P. Bedard and his group of RSMAS. We appreciate the help of G. Samuels and R. Zantopp (RSMAS) and of Dr. J. Fischer and M. Visbeck (IfM, Kiel) in the data analysis. We also thank Dr. J. Marshall (Imperial College, London) for helpful discussions. This study was supported by the National Science Foundation under Grant OCE 8614852.

REFERENCES

Bethoux, J.P., 1980: Mean water fluxes across sections in the Mediterranean Sea, evaluated on the basis of water and salt budgets and of observed salinities. *Oceanol. Acta,* **3,** 79–88.

Chereskin, T. K., E. Firing and J. A. Gast, 1989: Identifying and screening filter skew and noise bias in acoustic Doppler current profiler measurements. *J. Atmos. Oceanic Technol.,* **6,** 1040–1054.

Crépon, M., M. Boukthir, B. Barnier and F. Aikman III, 1989: Horizontal ocean circulation forced by deep-water formation. Part I: An analytical study. *J. Phys. Oceanogr.,* **19,** 1781–1792.

Gascard, J.-C., 1973: Vertical motions in a region of deep water formation. *Deep-Sea Res.,* **20,** 1011–1027.

——, 1978: Mediterranean deep water formation, baroclinic instability and oceanic eddies. *Oceanol. Acta,* **1,** 315–330.

——, and R. A. Clarke, 1983: The formation of Labrador Sea water. Part II: Mesoscale and smaller-scale processes. *J. Phys. Res.,* **13,** 1779–1797.

Hogg, N. G., 1973: The preconditioning phase of MEDOC 1969. Part II: Topographic effects. *Deep-Sea Res.,* **20,** 449–459.

Johns, W., 1988: Near-surface current measurements in the Gulf Stream using an upward-looking acoustic Doppler current profiler. *J. Atmos. Oceanic Technol.,* **5,** 602–613.

Killworth, P. D., 1976: The mixing and spreading phase of MEDOC 1969. *Progress in Oceanography,* Vol. 7, Pergamon, 59–90.

Leaman, K. D., and F. Schott, 1989: Hydrographic structure of the convection regime in the Gulf of Lions: Winter 1987. *J. Phys. Oceanogr.,* **21,** 573–596.

Madec, G., M. Chartier, P. Delecluse and M. Crépon, 1990: A three-dimensional study of deep-water formation in the northwestern Mediterranean Sea. *J. Phys. Oceanogr.,* in press.

MEDOC Group, 1970: Observation of formation of deep water in the Mediterranean. *Nature,* **227,** 1037–1040.

RD Instruments, 1989: Velocity measurement bias errors in the ADCP. RDI Tech. Bull. ADCP 89-06, 24 pp.

Sankey, T., 1973: The formation of deep water in the northwestern Mediterranean. *Progress in Oceanography,* Vol. 6, Pergamon, 159–179.

Schott, F., 1989: Measuring winds from underneath the ocean surface by upward-looking acoustic Doppler current profilers. *J. Geophys. Res.,* **94,** 8313–8321.

——, and W. Johns, 1987: Half-year long measurements with a buoy-mounted acoustic Doppler current profiler in the Somali Current. *J. Geophys. Res.,* **92,** 5169–5176.

——, K. Leaman and R. Zika, 1988: Deep mixing in the Gulf of Lions, revisited. *Geophys. Res. Letters,* **15,** 800–803.

Seung, Y. H., 1980: Low-frequency vertical motions in the MEDOC area of deep water formation. *Oceanol. Acta,* **3,** 441–447.

Swallow, J. C., and G. F. Gaston, 1973: The preconditioning phase of MEDOC 69. Part I: Observations. *Deep-Sea Res.,* **20,** 429–448.

Tauppier-Letage, I., and C. Millot, 1986: General hydrodynamical features in the Ligurian Sea inferred from the DYOME experiment. *Oceanol. Acta,* **9,** 119–131.

UNESCO, 1975: An intercomparison of some current-meters. Part III. SCOR WG 21, UNESCO Tech. Paper Marine Sci., **23,** 42 pp.

Voorhis, A. D., and D. C. Webb, 1970: Large vertical currents observed in a winter sinking region of the northwestern Mediterranean. *Cah. Oceanogr.,* **22,** 571–580.

Weller, R. A., J. P. Dean, J. Marra, J. F. Price, E. A. Francis and D. C. Boardman, 1985: Three-dimensional flow in the upper ocean. *Science,* **227,** 1552–1556.